Building Energy Efficiency Enhancement Through Load Reduction in the Air Conditioning System

Rahul Kumar Sharma[a], Ashish Kumar[a,b] and Dibakar Rakshit[a]

[a]Indian Institute of Technology Delhi, New Delhi (India)

[b]Galgotias University, Greater Noida (India)

Abstract

The humid and hot climate of the Indian Subcontinent steers air conditioning (AC) ownership. These conditions are made worse by global climate change and the "heat island effect". India's energy outlook report predicts growth in electricity consumption for cooling by sixfold to 650 TWh by 2040, more than Germany's total today, and accounts for more than half of all building electricity consumption. Further, with the onset of COVID-19, the health and air-conditioning societies have modified guidelines and suggested incorporating fresh air from ambient conditions to dilute the indoor air and reduce the contaminant level. Phase change materials provide constant temperature operation and store thermal energy. The present study aims to design a shell and tube heat exchanger to reduce a load of an HVAC system by cooling the fresh air from ambient temperature and subsequently mixed with the recirculated air of the AC unit. The fresh air at 315 K flows through the inner tube of the heat exchanger with calcium chloride hexahydrate filled in the annulus. Additionally, the effect of incorporating longitudinal internal fins into the inner tube of the heat exchanger on energy saving is investigated. The designed heat exchanger with no fin, fin of 50 mm height, and 75 mm height led to an average energy saving of 3%, 4.95% and 5.56%, respectively, for 3600 s of operation. The proposed system will provide a guideline to the sustainable solution pertaining to the issue of increasing energy consumption by the HVAC system, hence making buildings energy efficient.

Keywords: HVAC, Building Energy Efficiency, Phase Change Material, Heat Exchanger

1. Introduction

Buildings are an essential and integral part of the human race and account for 20% of the total energy usage in the world(Conti et al., 2016). Almost 60% of this energy demand in tropical regions is required to maintain human thermal comfort (Abu-Hamdeh et al., 2021). India, a developing country lying in the tropical climatic zone of the earth, expects a twofold increase in the building floor area in 2040 compared to the building floor area in 2021(Energy Agency, 2021). Further, the units of air conditioners installed are expected to increase to 1.6 units per household and will increase India's consumption of electricity for cooling to 650 TWh by 2040, which is more than the total electricity consumption of Germany today and accounts for around half of all electricity consumption in buildings (Energy Agency, 2021). Energy efficiency improvements in air conditioners, as well as thermally efficient building design, cool roofs, and the use of alternative more efficient cooling appliances such as desert air coolers, could help to reduce the increase in cooling demand.

Phase change materials (PCM) that work on the principle of latent energy storage have good energy storage capacity, operate at a constant temperature range, and can absorb thermal energy when the temperature is higher than the melting point. At the same time, release the heat when the temperature drops below the melting point temperature. Due to the aforementioned properties, studies have been found with active applications in the preservation of food and pharmaceutical products (Belman-Flores et al., 2015), solar cooling and solar power plants (Aydin et al., 2015), photovoltaic electricity systems (Ma et al., 2015), solar dryers in the agricultural industry (Shalaby et al., 2014) waste heat recovery systems (Fang et al., 2014), domestic hot water (Seddegh et al., 2015), and enhancing the energy performance and thermal comfort in buildings. PCM increases the thermal mass of the building envelope and helps in energy management (Verma et al., 2023). With this technique, the insulating envelope absorbs the heat and releases it when the outdoor temperature drops, leading to a shift and decrease in the peak indoor loads. Over the years, PCM has been used in buildings in different configurations. The application of PCM to ceiling panels effectively reduces energy consumption through active cooling systems (Yahaya & Ahmad, 2011). PCM used in brick walls reduced 24.32% of the cooling load for the PCM wall under summer conditions(Wang et al., 2016). Window glazing with PCM has effectively reduced the cooling load(Fasi & Budaiwi, 2015). PCM-air heat exchangers (PAHX) can provide an efficient and effective solution to the problem of ambient air at a higher temperature. Yanbing et al.(Yanbing et al., 2003) combined the PAHX system with a night ventilation strategy for the moderate climate of Beijing and

Selection and/or peer review under responsibility of Scientific Committee
doi:10.18086/eurosun.2022.01.12 Available at http://proceedings.ises.org

achieved a considerable enhancement in indoor thermal performance. Osterman et al.(Osterman et al., 2015) studied system thermal performance for free cooling and heating in Slovenia and observed its heating and cooling potential for different weather conditions.

The onset of COVID-19 affected human lives and the guidelines for cooling and heating the building envelopes. The Indian Society of Heating, Refrigerating and Air Conditioning Engineers (ISHRAE), American Society of Heating, Refrigerating and Air-Conditioning Engineers (ASHRAE) and health societies have suggested the incorporation of fresh air into closed spaces to dilute the air and reduce contamination levels in closed areas (Kapur et al., 2020; Washington State Department of Health, 2020). During the summer, the ambient temperature in Delhi may reach 315 K, as per the observation from the weather station at the Indian Institute of Technology Delhi. In typical air conditioners, the air from the room is recirculated to the air-conditioning unit (AC). However, when fresh air is introduced, a portion of the total air is replaced by the ambient air at ambient conditions, as illustrated in Figure 1. Hence it will further increase the energy consumption of the AC unit and thereby the energy consumed by a building (Kumar Sharma et al., 2022).

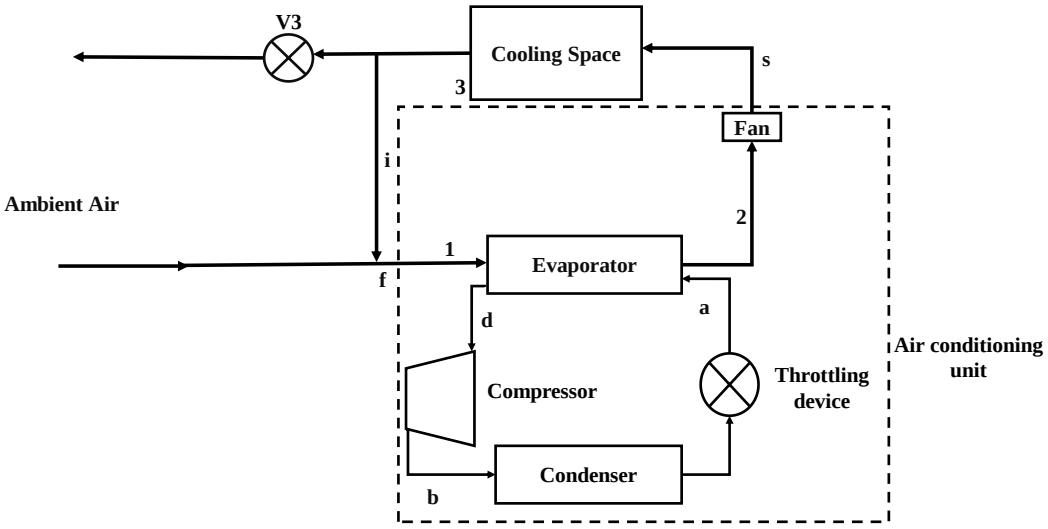

Figure 1 Schematic Layout of a conventional air-conditioning system with fresh air incorporation

The literature review has suggested the PCM capabilities to act as a thermal energy storage system and enhance buildings' energy efficiency via different designs and configurations. However, its application with the HVAC system in buildings is not being explored. The reports by various agencies indicate a steep rise in HVAC systems in the coming decades. The present numerical study uses a PCM-based shell and tube heat exchanger to make an AC system with fresh air incorporation more energy efficient. The heat exchanger is used to cool the fraction of ambient air before mixing it with the recirculation air, reducing the AC unit's cooling load and making it more energy efficient. Further, the effect of enhancing the heat transfer rates using fins is also analysed in the study. So the heat exchanger design is tested for three configurations, unfinned, 75 mm × 5 mm, and 50 mm × 5 mm, with six longitudinal fins.

2. Physical Domain

In the present study, a type of latent heat energy storage system (LHESS) is considered for cooling the air. The system is a simple shell and tube heat exchanger. The tube diameter is 200 mm, made of aluminium with a thickness of 5 mm and a shell diameter of 250 mm, while the heat exchanger length is 1500 mm, as shown in figure 2(a). The PCM considered for the study is calcium chloride hexahydrate, having a melting temperature of 30°C. Air flows through the heat exchanger and releases its thermal energy, which gets stored in the latent heat energy storage medium. Since the thermal diffusivity of air is low, six equidistant longitudinal internal fins are incorporated, which are placed at 60^{o} radial angle with two sets of fin dimensions, one of 50 mm height and 5 mm width, while the other has dimensions of 75 mm in height and 5 mm in width.

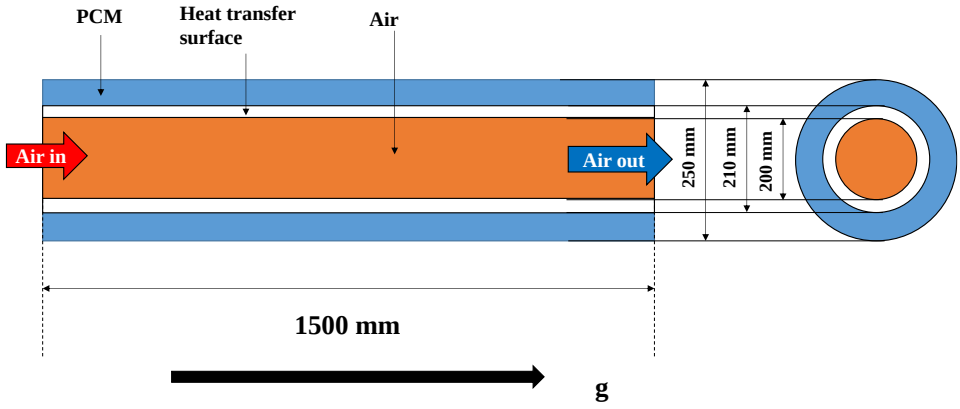

(a)

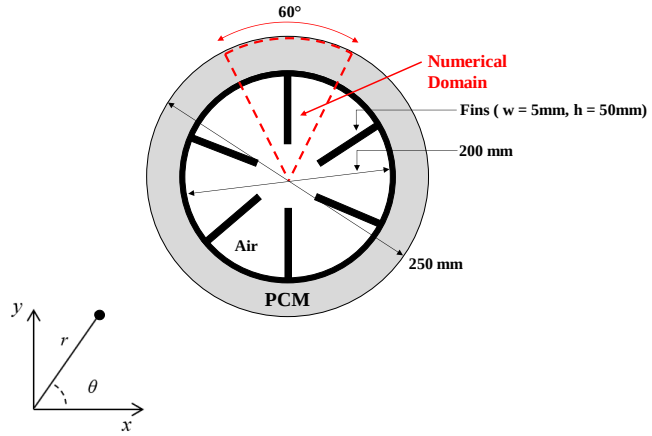

(b)

Figure 2: (a) Schematic of PCM-based shell and tube heat exchanger (b) Physical domain

To reduce the computational time and effort, the analysis is considered by considering one-sixth axisymmetric three-dimensional domain of the LHESS by imposing symmetrical boundary conditions and assuming a constant velocity at the inlet, as shown in figure 2(b). The considered axisymmetric case will replicate the heat transfer and flow phenomenon of the complete shell and tube heat exchanger. The thermophysical properties of calcium chloride hexahydrate, air and aluminium are mentioned in table 1. The velocity of the air inlet is fixed at 6 m/sec. After passing the air through the heat exchanger, the air is mixed with a fraction of recirculation air and fed to the AC unit. The AC unit works on a vapour compression refrigeration cycle with a compression ratio of 5 and maintains the office space at 300 K.

Table 1 Thermophysical properties of PCM, Air and Aluminium

Properties	**$CaCl_2.6H_2O$**(Das et al., 2021)	**Air**	**Aluminium**
c_p (kJ/kg.K)	2.230	1.006	8.710
ρ (kg/m^3)	1538	1.225	2719
k (W/m/K)	0.546	0.242	202.4
μ(kg/m.s)	0.1	1.789×10^{-5}	-
Latent heat(kJ/kg)	170	-	-
β (K^{-1})	0.0005	-	-
T_m (K)	303	-	-

3. Mathematical Modelling

A three-dimensional axisymmetric numerical model is used to solve the transient heat transfer and fluid flow in the shell and tube LHESS. An enthalpy porosity approach based on a fixed grid is used to illustrate the phase change behaviour of PCM. For the development of the numerical model, a few assumptions are made: (a) the phase change of the PCM occurs at a constant temperature, (b) the effect of expansion and contraction during the solidification and melting of PCM is excluded, and (c) the thermophysical properties of PCM, air, and pipe material are isotropic and temperature-invariant, except for the density of PCM in the direction of gravity (z-direction). The conservation equations for the PCM, air, and pipe are written in vector form as follows:

Continuity equation:

$$\frac{\partial(\rho_i)}{\partial t} + \nabla.(\rho_i V_i) = 0 \qquad \text{(eq. 1)}$$

Momentum equation:

$$\frac{\partial(\rho_i V_i)}{\partial t} + V_i \nabla.(\rho_i V_i) = -\nabla P + \nabla^2[\mu V_i] + AV_i + S_z \qquad \text{(eq. 2)}$$

Energy equation:

$$\frac{\partial(\rho_i c_{p,i} V_i)}{\partial t} + V_i \nabla.\left(\rho_i c_{p,i} V_i\right) = \nabla^2[k_i T_i] + S_{TP} \qquad \text{(eq. 3)}$$

Here i represent PCM, and for air, there is no source term and AV_i. In the case of the tube, only the energy equation is solved. The source term in the conservation of momentum equation for PCM represents the Boussinesq approximation in the z-direction, which assumes no change in thermophysical properties other than the fluid's density and can be expressed as :

$$S = \rho g \beta (T_p - T_m) \qquad \text{(eq. 4)}$$

Where β is the thermal expansion coefficient, and T_m is the melting temperature of PCM, while the parameter A can be represented as :

$$S = -A\frac{(1-\beta)^2}{\delta^3 + b} \qquad \text{(eq. 5)}$$

The source term in equation 3 is known as nodal latent heat revolution with time and is a function of temperature. The source term can be represented as :

$$S_{TP} = -\frac{\partial(\rho \Delta E)}{dt} \qquad \text{(eq. 6)}$$

ΔE represents the nodal heat value content, and its value varies from zero to latent heat of fusion.

In the present study, PCM is assumed to have the same solidus and liquidus temperatures. After the energy is transferred from the air to PCM through the aluminium finned/unfinned surface, the air is fed to the AC unit.

Initial and boundary conditions –

To minimise the sensible heating of PCM before melting, the initial temperature condition in the present study is considered relatively lower than the melting point of the PCM. The initial temperature condition can be expressed numerically as:

$$T(r,\theta,z,0) = 315\ K \qquad \text{(eq. 7)}$$

The boundary condition to solve the mass, momentum and energy conservation equation for air and PCM zone are :

(a) For the air domain:

(i) u = 0, at wall

(ii) z = 0, $u_z = u_{in}$ and $T_z = T_{in}(t)$ at inlet

(iii) p = 0 at outlet

(b) For the PCM domain:

(i) u = 0, at wall

(ii) At θ = -30˚ and θ = 30˚, symmetric boundary condition is imposed. i.e. $\frac{\partial \phi}{\partial n}\Big|_{sym} = 0$ and $\phi.\vec{n} = 0$

where, ϕ is either u or T and n is the unit vector normal to the surface.

3.1 Solution procedure

The governing equations (2), (3), (4) are iteratively solved using the Finite Volume Method (FVM), and the SIMPLE scheme is used for pressure-velocity coupling. The spatial discretisation of momentum and energy equations is carried out using power law. Ansys Fluent V2021 is a commercially available software to solve governing equations with suitable initial and boundary conditions. The convergence criteria for momentum and energy equation are set to 10^{-3} and 10^{-6}, respectively.

3.2 Energy content

The energy in the LHESS stored is stored in the form of latent heat and sensible heat, and their estimation is based on the average PCM temperature and the liquid fraction of PCM. Equations 8 and 9 can be used to calculate the total sensible heat and latent heat during the energy storage process :

$$Q_{sensible} = \sum_{t=0}^{t}(T^{t}_{avg,p} - T^{t-1}_{avg,p}) \quad \text{(eq. 8)}$$

$$Q_{sensible} = \sum_{t=0}^{t} mL_{latent}(\epsilon^{t} - \epsilon^{t-1}) \quad \text{(eq. 9)}$$

where m is the mass of PCM in the heat exchanger, t is the total time of operation, $t_{avg,p\ is}$ the average PCM temperature, and ϵ is the liquid fraction of PCM.

3.3 Energy consumption by Air-Conditioning system

The conventional AC system with fresh air incorporation is illustrated in figure 1. The AC system operates on a vapour compression and refrigeration (VCR) system. The temperature of the air inside the office space is managed as per the ISHRAE standards, i.e. 300 K DBT and relative humidity of 50% (Indoor, Quality, and Second 2019; Kapur et al. 2020; Refrigeration and Air Conditioning). The fresh air and the recirculated air mix adiabatically before entering the AC unit (Refrigeration and Air Conditioning;).

The total sensible heat extracted from the space (Qs) is given as :

$$Q_s = \dot{m}_a(1.005 + 1.88\omega)(T_{mix} - T_s) \quad \text{(eq. 10)}$$

Here $\dot{m}_a$ is the total mass of air and calculated as :

$$\dot{m}_a = \dot{m}_{ai} + \dot{m}_{ao} \quad \text{(eq. 11)}$$

The present study supplies a 0.42 kg/s mass to cool the office space.

The enthalpy(h_{mix}) and temperature(T_{mix}) of the mixture of air obtained by :

$$h_{mix} = \frac{\dot{m}_{ai}h_i + \dot{m}_{ao}h_{out}}{\dot{m}_{ai} + \dot{m}_{ao}} \quad \text{(eq. 12)}$$

$$T_{mix} = \frac{\dot{m}_{ai}T_i + \dot{m}_{ao}T_o}{\dot{m}_{ai} + \dot{m}_{ao}} \quad \text{(eq. 13)}$$

The load on the chiller ($Q_{chiller}$) is dependent on the temperature of mixed air, and the supply air temperature is estimated as :

$$Q_{chiller} = \dot{m}_a(h_1 - h_s) \quad \text{(eq. 14)}$$

$Q_{chiller}$ then determines the mass of the refrigerant required to achieve the desired refrigeration effect.

$$\dot{m}_{ref} = \frac{Q_{chiller}}{(h_a - h_d)} \quad \text{(eq. 15)}$$

Since in a VCR system, the compressor is the primary energy-consuming unit, so for the study, we have assumed the total energy consumed by the AC system corresponds to the energy consumed by the compressor in the system. The work required by the compressor is given by :

$$W_{comp} = \dot{m}_{ref}(h_{bs} - h_d) \quad \text{(eq. 16)}$$

The compressor's efficiency is a function of its operating pressures (Barthwal et al., 2021), hence calculating the work required by the AC system :

$$\eta_{comp} = \frac{h_{bs} - h_d}{h_b - h_d} = 0.85 - 0.046667\frac{p_2}{p_1} \quad \text{(eq. 17)}$$

$$W_{ac} = {}^{W_{comp}}/_{\eta_{comp}} \quad \text{(eq. 18)}$$

3.4 Grid Independence Test

A grid independence study for the designed LHESS is conducted to determine an appropriate grid size. To find the most suitable size, a coarse, fine and finer grid with the number of cells rising by a factor of two is studied. The coarse grid contains 354806 cells, whereas the fine and finer grids have 685350 and 1211560 cells, respectively. In the computational domain, the average output air temperature variation with time from the heat exchanger is compared at different mesh sizes. The maximum divergence of average outlet air from heat exchanger temperature during charging is 0.16 K when the number of cells is amplified from 354806 to 685350 and 0.014 K for an increase in the number of cells from 685350 to 1211560. As a consequence of this study, the fine grid can be considered for future investigations. Because the difference in temperature distribution in LHESS becomes minor as the time step is reduced further, the time step is set at 0.1 s.

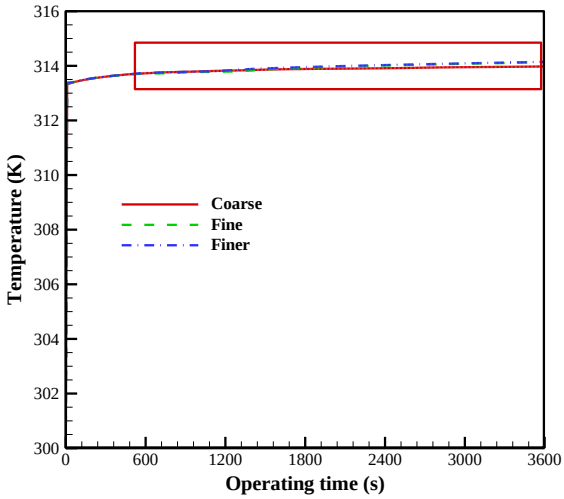

Figure 3: Grid Independence Study

4. Results and Discussion

4.1 Melting Fraction

The heat transfer characteristics of the shell and tube heat exchanger while the charging process is discussed, followed by the energy savings achieved by retrofitting the heat exchanger into an AC system. The fins of height 50 mm and 75 mm are considered in the inner tube of the shell and tube configuration, and the performance is compared with an unfinned tube. The temporal variation of the melting fraction for the three different configurations on the inner tube in the heat exchanger is illustrated in Figure 4. The melting process indicates that the thermal energy from the air gets absorbed into the phase latent energy storage medium in the heat exchanger. It can be observed from the figure that the melting of the PCM starts after 180 s of the charging process for the unfinned inner tube. However, with the addition of six internal fins in the inner tube, the onset time of PCM melting reduces. For six longitudinal fins of a height of 50 mm and width of 5 mm running through the heat exchanger, the start of the melting process is noticed after 122 s of changing process. This is because of an increase in the heat transfer area and consequently the heat transfer rate due to internal fins. The increase in the height of the internal fins to 75 mm while keeping the width and the number of fins constant further reduces the beginning of the melting process of PCM to 80 s. In the charging process, one hour of operation is considered; it is observed that complete melting of PCM is achieved at 2960 s and 2910 s for the cases with 50 mm and 75 mm fin configuration, while some portion of PCM remains unmelted in the heat exchanger with no fin.

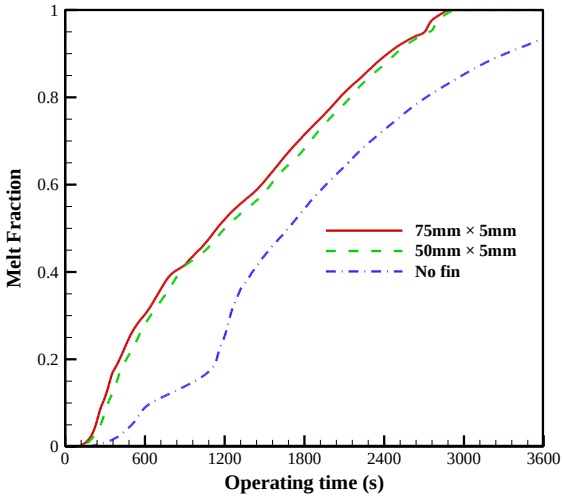

Figure 4: Melt fraction variation with time for different configurations of the heat exchanger

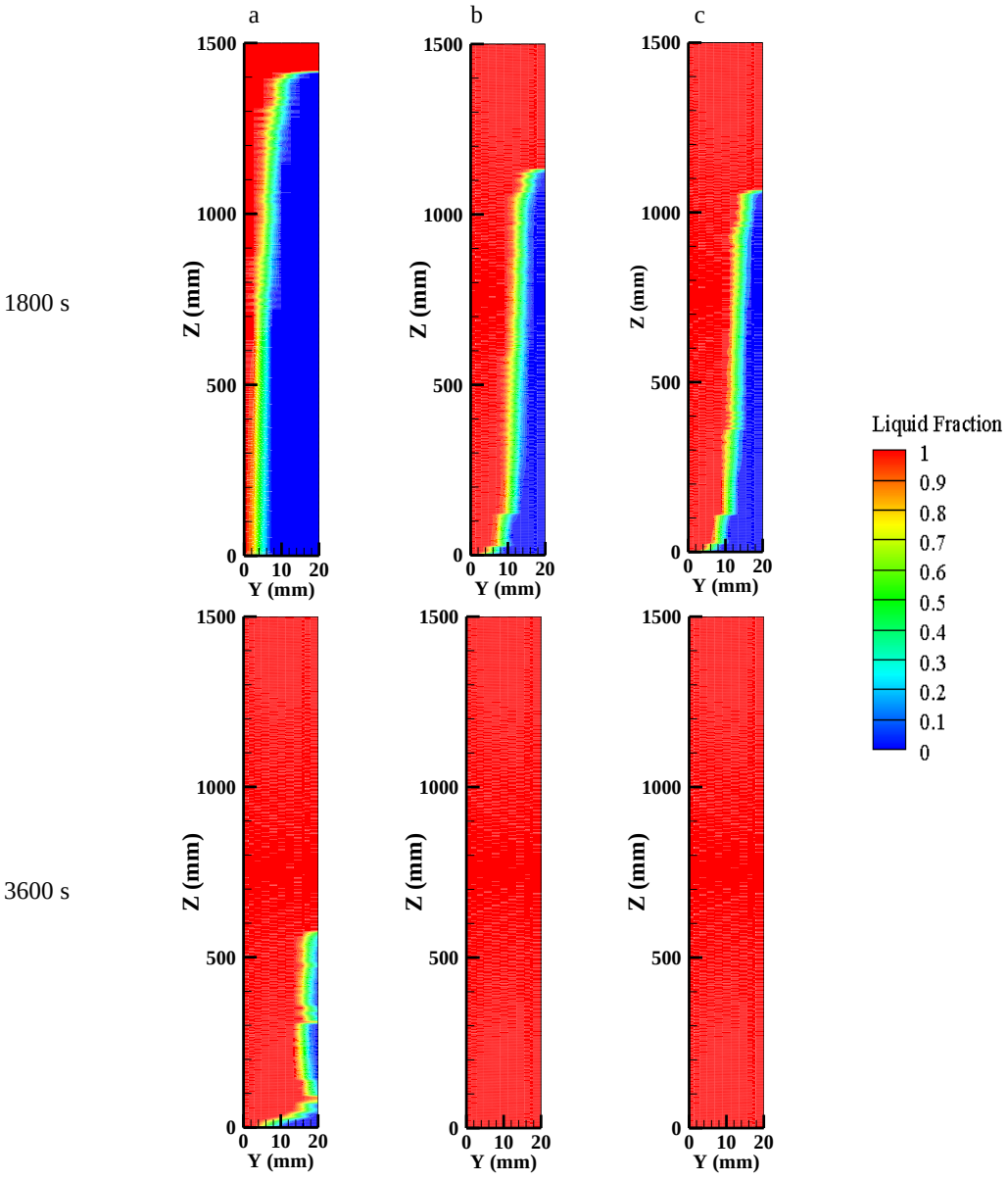

Figure 5: Melting fraction for a) no fin, b) six fins of 50 mm × 5 mm, and c) six fins of 75 mm × 5 mm

Further, the melting profile is observed from the melt front contours at the time instances of 1800 s and 3600 s of charging, as shown in figure 5. From the contour of melted PCM for a heat exchanger without fins, it can be observed that after 1800 s, the melted PCM in the upper portion of the heat exchanger is higher than in the lower part. The behaviour in melting is due to the dominance of conduction in the initial phase of operation. With time the convection currents also enhance the heat transfer within the fluid. Due to the buoyancy effect and temperature difference, the melted PCM rises upwards, and the heat transfer phenomenon occurs due to natural convection. Further, after 3600 s, the melt fraction of the PCM increases from 54.5% after 1800 s to 93.5%.

Figure 5 (b) shows the melt front for 50 mm × 5 mm fin configuration, and it is found that after 1800 s of operation, the PCM melt fraction increases to 68.23% as compared to 54.5% melt fraction in no fin condition. The PCM melts completely after 2960 s; hence, the energy storage in latent heat ceases, and sensible heating dominates afterwards. In the case of 75 mm height of internal fins, it can be observed from figure 5 (c) that after 1800 s, the PCM melt fraction is 71.4%, which is increased to 100% before the end of the charging process. The fins effectively increase the heat transfer rate, which is evident from the melting fraction contours demonstrated in figure 5. When compared to unfinned, six fins of 50 mm height and 5 mm width increase the melting rate and at a time instance of 1800 s, an enhancement of 13.73%, while for the fins of 75 mm height and 5 mm width, the melting is further increased by 16.9%. The increase in melting fraction rate is highest for the heat exchanger with six fins of 75 mm height and 5 mm width and least for the heat exchanger with no fins.

4.2 Air outlet temperature

The air temperature at the outlet temperature varies with operation time and is illustrated in Figure 5. The rate of increase in air temperature is high for the initial 300 s temperature, and after that, it is constant. For the heat exchanger with no fin, the air temperature at the outlet of the heat exchanger has fewer fluctuations, with an average temperature reduction of 1.25 K and 1.09 K for 1800 s and 3600 s, respectively.

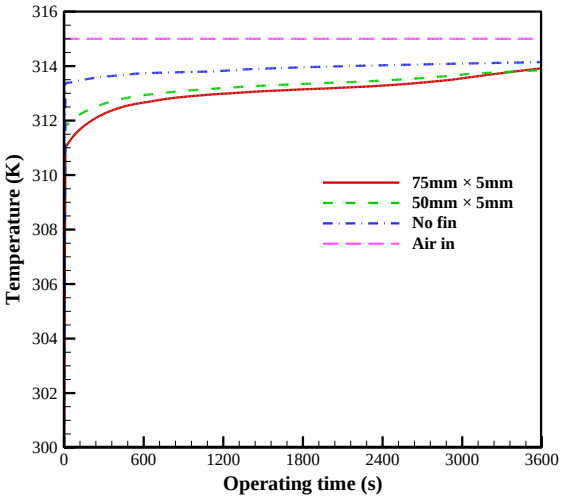

Figure 6: Temporal variation in air temperature at the outlet for different configurations of the heat exchanger

The 50 mm × 5 mm fin configuration achieved a more significant drop in air temperature at the heat exchanger outlet when compared with the unfinned configuration. The reduction in air temperature is 2.03 K and 1.74 K after 1800 s and 3600 s, respectively. The air temperature is reduced by 63.55% and 57.8% compared to the heat exchanger with no fins after 1800 s and 3600 s, respectively. The air temperature profile in figure 6 indicates the air temperature reduction in the proximity of fins.

Further increasing the dimension of the fin to 75 mm × 5 mm, the temperature reduced to 2.31 K and 1.93 K after 1800 s and 3600 s, respectively. Hence, increasing the reduction further by 86.23% and 76.78% for the air temperature with no fins after 1800 s and 3600 s, respectively. While the air temperature drop obtained from 75mm fins is 12% more compared to the fins with 50 mm height.

Time a b c

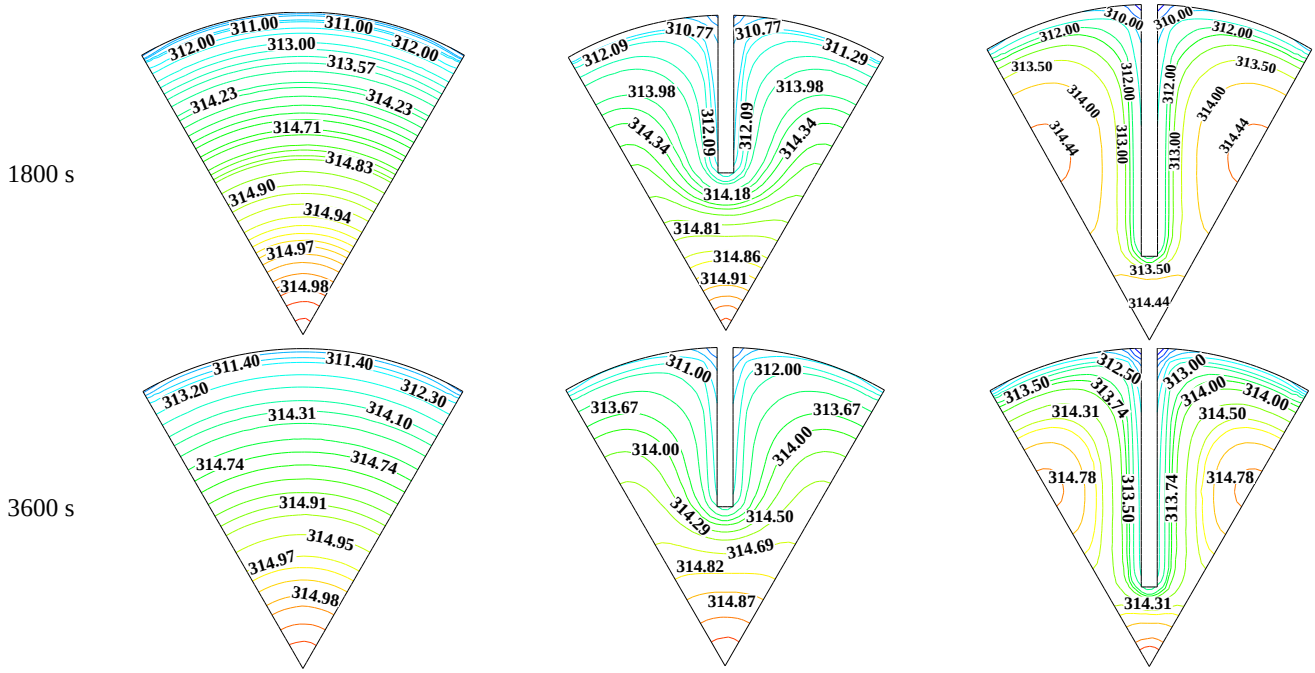

Figure 7: Air temperature at the outlet for a) no fin, b) six fins of 50 mm × 5 mm, and c) six fins of 75 mm × 5 mm

In a VCR cycle compressor is the major energy-consuming component of the system. Hence, the energy saving is estimated through compressor load for the cases with VCR connected to the proposed heat exchanger unit compared to a non-retrofitted AC unit. The temporal variation of energy saved by using the heat exchanger is shown in figure 8. For the first 180 s, 100 s and 90 s in the heat exchangers with no fin, 50 × 5 and 75 × 5 fins, respectively, the energy saving is not estimated because of marginal heat transfer between air and PCM. For an unfinned shell and tube heat exchanger, a maximum energy savings of 3.57% is achieved at 180 s. The energy savings decrease with time, and the system achieves an average energy savings of 2.74% for the operation of 3600 s. The heat exchanger, with six fins of dimension 50 mm × 5 mm, has a maximum and average energy savings of 6.11% and 4.95% for 100 s and 3600 s, respectively. Further a maximum energy saving of 7.11% is achieved for the heat exchanger with six longitudinal fins of 75 mm height and 5 mm width, while the average energy saving is 5.56% for 3600 s. Among the three configurations, the heat exchanger with six fins of 75 mm × 5mm saves maximum energy compared to an AC system without a heat exchanger.

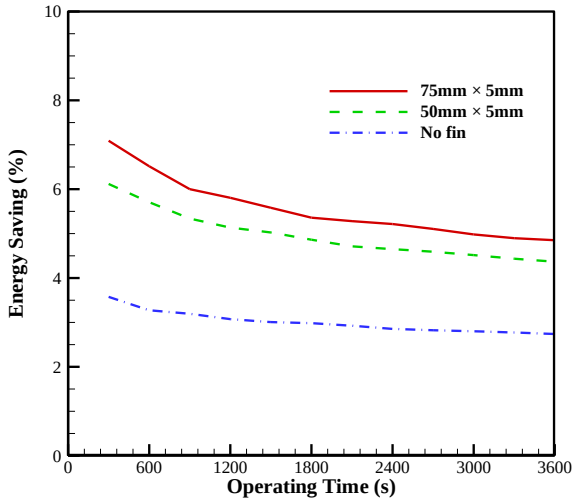

Figure 8: Energy saving by retrofitting air conditioner with different heat exchangers

Conclusions

A strategy to reduce the energy consumption of an AC unit using 50% fresh air per circulation is studied. The AC system is based on the VCR cycle and operates for 3600 s with ambient air supplied at a temperature of 315 K. To reduce the temperature of the fresh air provided at ambient conditions a PCM-based shell and tube heat exchanger with a PCM thickness of 20 mm is designed. The fresh air flows through it, and PCM stores the thermal energy in latent heat. The heat transfer performance of the heat exchanger is analysed, and its effect on energy consumed is studied. It is found that a shell and tube heat exchanger provided an average outlet air temperature reduction of 1.09 K for 3600 s of operation. Incorporating this heat exchanger into a VCR-based AC system leads to a peak and average energy savings of 3.57% and 3%, respectively, for 3600 s. Additionally, the effect of extruding fins on the air side of a heat exchanger is explored. The modified heat exchangers have six longitudinal fins running through the length of the heat exchanger with a width of 5 mm and height of 75 mm and 50 mm. The incorporation of internal fins in the heat exchanger increases the energy saving of the VCR system through further reduction of air outlet temperature. However, it is observed that due to the fast melting rate in the presence of internal fins, sensible heating dominates after the complete melting of PCM. This results in a slight reduction in energy saving with the increase in charging time. It is found that the longitudinal internal fins of a width of 5 mm in the inner pipe of the heat exchanger, attributed to enhancement in the temperature drop by 76.78% and 57.5% for fins of height 75 mm and 50mm, respectively. The proposed system will provide an effective solution to the ever-increasing energy demand for the AC system. The study will serve as a guide in designing a PCM heat exchanger with VCR systems.

Acknowledgments

The authors thank HPC facility at IIT Delhi for computational resources. The second author acknowledges the Institute Postdoctoral fellowship. The author also acknowledges the Department of Science and Technology, Government of India "Different Energy Vector Integration for Storage of Energy" - Grant number- TMD/CERI/MICALL19/2020/03(G). The first author would like to thank IIT Delhi for providing the travel assistance- Grant number- IITD/PGSR/2022/67206.

Nomenclature

List of Acronyms			
AC	Air conditioning	HVAC	Heating Ventilation and Air Conditioning
DBT	Dry bulb temperature	LHESS	Latent Heat Energy Storage System
HTF	Heat Transfer Fluid	VCR	Vapour Compression Refrigeration
PCM	Phase Change Material		

List of Symbols			
A	Contact Area (m^2)	h	Enthalpy per kg (kJ/kg)
Q	Heat Flow Rate (W)	k	Thermal Conductivity (K/W)
T	Temperature (K)	$\dot{m}$	Mass Flow Rate (kg/s)
W	Work Done (W)	p	Pressure (Pa)

List of subscripts			
a	Ambient	mix	Mixed Air
avg	Average	ref	Refrigerant
comp	Compressor	s	Supply Air

Greek Letters			
η	efficiency	μ	Viscosity (kg/m.s)
ρ	density (m3/kg)	β	thermal expansion coefficient (K^{-1})

References

Abu-Hamdeh, N. H., Melaibari, A. A., Alquthami, T. S., Khoshaim, A., Oztop, H. F., & Karimipour, A. (2021). Efficacy of incorporating PCM into the building envelope on the energy saving and AHU power usage in winter. *Sustainable Energy Technologies and Assessments*, *43*, 100969. https://doi.org/10.1016/J.SETA.2020.100969

Aydin, D., Casey, S. P., & Riffat, S. (2015). The latest advancements on thermochemical heat storage systems.

Renewable and Sustainable Energy Reviews, *41*, 356–367. https://doi.org/10.1016/J.RSER.2014.08.054

Belman-Flores, J. M., Barroso-Maldonado, J. M., Rodríguez-Muñoz, A. P., & Camacho-Vázquez, G. (2015). Enhancements in domestic refrigeration, approaching a sustainable refrigerator – A review. *Renewable and Sustainable Energy Reviews*, *51*, 955–968. https://doi.org/10.1016/J.RSER.2015.07.003

Conti, J., Holtberg, P., Diefenderfer, J., LaRose, A., Turnure, J. T., & Westfall, L. (2016). *International Energy Outlook 2016 With Projections to 2040*. https://doi.org/10.2172/1296780

Das, D., Sharma, R. K., Saikia, P., & Rakshit, D. (2021). An integrated entropy-based multi-attribute decision-making model for phase change material selection and passive thermal management. *Decision Analytics Journal*, *1*, 100011. https://doi.org/10.1016/J.DAJOUR.2021.100011

Energy Agency, I. *India Energy Outlook 2021 World Energy Outlook Special Report*. Retrieved September 7, 2022, from www.iea.org/t&c/

Fang, G., Tang, F., & Cao, L. (2014). Preparation, thermal properties and applications of shape-stabilized thermal energy storage materials. *Renewable and Sustainable Energy Reviews*, *40*, 237–259. https://doi.org/10.1016/J.RSER.2014.07.179

Fasi, M. A., & Budaiwi, I. M. (2015). Energy performance of windows in office buildings considering daylight integration and visual comfort in hot climates. *Energy and Buildings*, *108*, 307–316. https://doi.org/10.1016/J.ENBUILD.2015.09.024

Kapur, V., Agarwal, B., Baliga, G., Bhambure, J. M., Garg, V., Mathur, J., Mittal, R., Murthy, V., Rajasekaran, S., Shukla, Y., & Sur, A. (2020). ISHRAE COVID-19 Guidance Document for Air Conditioning and Ventilation. *Indian Society of Heating, Refrigerating & Air Conditioning Engineers*, 15.

Kumar Sharma, R., Yagnamurthy, S., & Rakshit, D. (2022). Energy analysis of a phase change material embedded heat exchanger for air conditioning load reduction in different Indian climatic zones. *Sustainable Energy Technologies and Assessments*, *53*, 102776. https://doi.org/10.1016/J.SETA.2022.102776

Ma, T., Yang, H., Zhang, Y., Lu, L., & Wang, X. (2015). Using phase change materials in photovoltaic systems for thermal regulation and electrical efficiency improvement: A review and outlook. *Renewable and Sustainable Energy Reviews*, *43*, 1273–1284. https://doi.org/10.1016/J.RSER.2014.12.003

Osterman, E., Butala, V., & Stritih, U. (2015). PCM thermal storage system for 'free' heating and cooling of buildings. *Energy and Buildings*, *106*, 125–133. https://doi.org/10.1016/J.ENBUILD.2015.04.012

Seddegh, S., Wang, X., Henderson, A. D., & Xing, Z. (2015). Solar domestic hot water systems using latent heat energy storage medium: A review. *Renewable and Sustainable Energy Reviews*, *49*, 517–533. https://doi.org/10.1016/J.RSER.2015.04.147

Shalaby, S. M., Bek, M. A., & El-Sebaii, A. A. (2014). Solar dryers with PCM as energy storage medium: A review. *Renewable and Sustainable Energy Reviews*, *33*, 110–116. https://doi.org/10.1016/J.RSER.2014.01.073

Verma, R., Kumar, S., Rakshit, D., & Premachandran, B. (2023). Design and Optimization of Energy Consumption for a Low-Rise Building With Seasonal Variations Under Composite Climate of India. *Journal of Solar Energy Engineering*, *145*(1). https://doi.org/10.1115/1.4054831

Wang, X., Yu, H., Li, L., & Zhao, M. (2016). Experimental assessment on the use of phase change materials (PCMs)-bricks in the exterior wall of a full-scale room. *Energy Conversion and Management*, *120*, 81–89. https://doi.org/10.1016/J.ENCONMAN.2016.04.065

Washington State Department of Health. (2020). *Ventilation and Air Quality for Reducing Transmission of COVID-19*. *19*(October 27, 2020), 1–4.

Yahaya, N. A., & Ahmad, H. (2011). Numerical Investigation of Indoor Air Temperature with the Application of PCM Gypsum Board as Ceiling Panels in Buildings. *Procedia Engineering*, *20*, 238–248. https://doi.org/10.1016/J.PROENG.2011.11.161

Yanbing, K., Yi, J., & Yinping, Z. (2003). Modeling and experimental study on an innovative passive cooling system—NVP system. *Energy and Buildings*, *35*(4), 417–425. https://doi.org/10.1016/S0378-7788(02)00141-X